Atmos. Chem. Phys. Discuss., 14, 16123–16149, 2014
www.atmos-chem-phys-discuss.net/14/16123/2014/
doi:10.5194/acpd-14-16123-2014

Atmospheric Chemistry and Physics
Discussions
Open Access

The distribution and trends of fog and haze in the North China Plain over the past 30 years

G. Q. Fu[1,3], W. Y. Xu[2], R. F. Rong[1], J. B. Li[4], and C. S. Zhao[2]

[1]Hebei Province Meteorological Service Centre, Shijiazhuang, Hebei, China
[2]Department of Atmospheric and Oceanic Sciences, School of Physics, Peking University, Beijing, China
[3]Key Laboratory for Meteorology and Ecological Environment of Hebei Province, Shijiazhuang, Hebei, China
[4]Hebei Province Meteorological Observatory, Shijiazhuang, Hebei, China

Received: 29 April 2014 – Accepted: 12 June 2014 – Published: 19 June 2014

Correspondence to: C. S. Zhao (zcs@pku.edu.cn)

Published by Copernicus Publications on behalf of the European Geosciences Union.

Abstract

Frequent low visibility, haze and fog events were found in the North China Plain (NCP). Data throughout the NCP during the past 30 years were examined to determine the horizontal distribution and decadal trends of low visibility, haze and fog events. The impact of meteorological factors such as wind and RH on those events was investigated. Results reveal distinct distributions of haze and fog days, due to their different formation mechanisms. Low visibility, haze and fog days all display increasing trends of before 1995, a steady stage during 1995–2003 and a drastically drop thereafter. All three events occurred most frequently during the heating season. Benefiting from emission control measures, haze and fog both show decreasing trends in winter during the past 3 decades, while summertime haze displays continuous increasing trends. The distribution of wind speed and wind direction as well as the topography within the NCP has determinative impacts on the distribution of haze and fog. Weakened south-easterly winds in the southern part of the NCP has resulted in high pollutant concentrations and frequent haze events along the foot of the Taihang Mountains. The orographic wind convergence zone in the central band area of the southern NCP is responsible for the frequent fog events in this region. Wind speed has been decreasing throughout the entire southern NCP, resulting in more stable atmospheric conditions and weaker dispersion abilities, calling for harder efforts to control emissions to prevent haze events. Haze events are strongly influenced by the ambient RH. RH values associated with haze days are evidently increasing, suggesting that an increasing fraction of haze events are caused by the hygroscopic growth of aerosols, rather than simply by high aerosol loadings.

ACPD
14, 16123–16149, 2014

1 Introduction

Low visibility events caused by fog and severe haze events can be a heavy burden for air transport and on-road traffic. The severe aerosol pollution that has led to the visibility impairment is also highly damaging for human health.

In developed countries such as the US and the European countries, the employment of sulphur emission control measures have already resulted in significant declines in haziness and major improvements in visibility during the past 50 years (Schichtel et al., 2001; Doyle and Dorling, 2002; Molnár et al., 2008; Vautard et al., 2009). As a rapidly developing country, however, air pollution problems has been haunting China for the past few decades. Visibility has been deteriorating in southeast (Deng et al., 2012) and southwest China (Fu and Wu, 2011) during the past 50 years, with only a few places revealing slight increases in recent years. Six Chinese mega-cities have suffered from continuously decreasing visibilities in the past 30 years (Chang et al., 2009). Overall, sunny day visibilities decreased significantly during 1960–1990 all over China, trends thereafter, however, were not coherent (Wu et al., 2012).

The visibility trends were often attributed to the variation of sulphur dioxide emissions or aerosol concentrations, however, no causality could be established so far. Both SO_2 and aerosol pollution have been proved most severe in the North China Plain (NCP), due to the rapid economic growth and the high population density (Xu et al., 2011). As a result, low visibility events frequently occur. Many in-situ measurements and studies have already been performed to study the light scattering properties of aerosols and their impact on horizontal visibility under different relative humidity (RH) in the NCP as part of the Haze in China (HaChi) Campaign (Chen et al., 2012; Ma et al., 2011). Results show that under low RH, low visibility events are mostly induced by the heavy aerosol loading, while under high RH, the influence of aerosol hygroscopic growth becomes stronger and can lead to low visibility events even under moderate aerosol pollution levels. However, only few studies have been performed to investigate the spatial distribution of low visibility events and their overall variation trend during the past few decades in the NCP. (Zhao et al., 2011) analysed the visibility trends in the NCP, suggesting declining visibilities before 1998 and increasing ones during 2006–2008, with stronger visibility deterioration trends in the summer season due to higher RH and lower wind speeds. Both haze and fog events could be the responsible for low visibility events, however, those were rarely differentiated in the study of visibility trends, which made it difficult to find the reason behind those visibility variations.

In this study, a detailed analysis on the decadal variation and spatial distribution of low visibility, fog and haze events in the most polluted southern part of the NCP will be performed and the impact of wind and RH on those events will be revealed.

2 Data and methodology

The North China Plain (NCP) is surrounded to the north by the Yan Mountains, to the west by the Taihang Mountains and to the east by the Bohai Sea (Fig. 1). The western part of the NCP is affected by the warm and dry wind coming off the eastern Taihang Mountain slopes, which lead to increased surface stability. Under the influence of the Bohai Sea, the east coast of the NCP often experiences large winds. The southern part of the NCP is rather flat and is an important water vapour transport passageway.

The location of the 64 meteorological observation sites selected for this study are displayed in Fig. 1, with the names of the sites given in Fig. 2a. All sites are located in the southern part of the NCP, where the air pollution is most severe. The visibility, RH, wind speed and weather phenomenon observed at 14:00 LT during 1981–2010 was used to analyse the long-term temporal and spatial variation of low visibility, haze and fog events.

Both haze and fog could lead to low visibility events. The formations of haze and fog are two distinctly different processes. Therefore, it is necessary to differentiate between those two events when analysing low visibility trends, distributions and variations. In this work, low visibility events were defined as days with visibility at 14:00 LT below 10 km. Those low visibility events that were not associated with fog, precipitation, dust storm,

ACPD
14, 16123–16149, 2014

smoke, snow storm etc. were defined as haze events. Fog events mostly occur during early morning, rarely lasting until 14:00 LT. Therefore, a day was defined as a foggy day if the occurrence of fog was recorded at any time during the day.

For each station the total occurrences of low visibility days, hazy days and foggy days during 1981–2010 were counted to analyse the spatial distribution of those 3 events. OMI Level 3 SO_2 planetary boundary layer column concentrations during 2005–2012 were used to show the correlation between the distribution of SO_2 and the occurrence of haze days.

The spatial average annual and 10 year moving average occurrence frequencies during 1981–2010 were used to analyse the trend of the 3 events over those 30 years. The variation trends are then compared to the SO_2 emission trends inferred from the China statistical yearbooks (National Bureau of Statistics of China, 1995–2010). The spatial average monthly occurrence frequencies during 1981–2010 were applied to examine the long-term trend of those 3 events in different seasons.

The average distribution and the linear trend of wind speeds during 1981–2010 were respectively calculated to reveal their impact on the distribution and variation trend of the occurrence frequency of the 3 events. NCEP final analysis meteorology data during a continuous fog event in between 9 and 19 December 2002 was used to reveal the characteristic wind field that has led to fog events in the southern NCP. Surface automatic weather station wind data during May–December 2009 were used as supplements to analyse the distribution of the wind field in the entire NCP and how it impacts on haze formation.

The average distribution of all RH and the haze related RH were calculated to show its relation to the distribution of low visibility, haze and fog events. To further study the influence of RH on haze events, the decadal variation of the ratio of the annual average haze related RH to the total average RH was compared against the decadal variation in annual haze days. The season-decadal variation trend of the occurrence frequency of haze related RH values falling in the range of RH $< 50\,\%$, $50\,\% <$ RH $< 60\,\%$,

ACPD
14, 16123–16149, 2014

60 % < RH < 70 %, RH > 70 % was analysed to show the impact RH has on haze in different seasons.

3 Results and discussions

3.1 The spatial distribution of low visibility, haze and fog

Low visibility, haze and fog events are formed through different mechanisms, hence their occurrences are determined by different parameters. This may lead to distinct spatial distributions of occurrence frequencies. The spatial distributions of the counts of low visibility, haze and fog days during 1981–2010 in the southern NCP are respectively depicted in Fig. 2b–d.

Haze events are caused by either high aerosol loadings or the strong hygroscopic growth of aerosols. SO_2 is the main precursor of sulphate aerosols, which are highly hygroscopic and exist in abundance in the NCP (Liu et al., 2014). The average SO_2 planetary boundary layer (PBL) column amount during 2005–2012 is depicted in Fig. 2a. High SO_2 column concentrations are found on the western border, which is caused on the one hand by the large amount of SO_2 emissions in this region and on the other hand by the special topography which has led to poor dispersion conditions. The high SO_2 concentrations have led to large loadings of highly hygroscopic sulphate aerosol, which can easily lead to haze events in this region. Figure 2c displays the distribution of the count of haze days, which shows a very similar distribution to that of SO_2 column concentration. Haze also most frequently occurs on the western border of the NCP, along the eastern slope of the Taihang Mountains.

The count of fog days show a very distinct distribution to that of haze days (Fig. 2d). Fog events most commonly occur along the centre line of the plain region, parallel to the southwest-northeast ridge of the Taihang Mountain. This suggests that the formation of haze and fog are controlled by different physical processes. While the formation of haze mainly depends on the local aerosol pollution level, the formation of fog is not limited

ACPD
14, 16123–16149, 2014

the existence of cloud condensation nucleus under the regional pollution state of the NCP. The special topography and meteorology in the NCP could be the responsible for the spatial distribution of fog event occurrences, which will be further discussed in Sect. 3.3.2.

Low visibility events can be caused by both haze and fog. The area with the most low visibility days covers both the area with the most haze and fog days. Low visibility mainly happens in the western part of the region, which is similar to the distribution of haze days. High centres were found around the three major cities Shijiazhuang, Xingtai and Handan. This indicates that low visibility events in the NCP are mostly caused by haze, rather than by fog.

Due to the distinct spatial distribution of low visibility, haze and fog days, the spatial coverage of their influence also differ from each other. Table 1 lists the number (percentage) of stations under various count ranges of low visibility, haze and fog days during 1981–2010. In the southern NCP, 34 % and 36 % of the stations have respectively observed 500–999 and 1000–1999 low visibility days, while another 12 % of the stations have gone through more than 2000 low visibility days and 17 % rather clean stations have only had 100–499 low visibility days. Although haze events can be very frequent, its impact is constrained within the limited area in the southwest. 22 % of the sites have experienced more than 1000 haze days during the past 30 years, while 55 % of the sites have had less than 500 haze days. For fog events, however, 73 % of the sites have experienced 500–999 fog days during the past 30 years, suggesting that a large area is under a similar influence of fog events.

In all, low visibility, haze and fog days are distinctly distributed in the NCP, because their formations are controlled by different mechanisms. The spatial distribution of haze days is determined by the distribution of pollutant emissions and by the topography of the NCP, thus only influencing a small area near the edge of the mountains. The distribution of fog days is mainly determined by the topography and meteorology, affecting a large area parallel to the mountains. Low visibility is mostly induced by haze events, thus showing a similar distribution to that of haze days.

ACPD
14, 16123–16149, 2014

3.2 The trends of low visibility, haze and fog during 1981–2010

The temporal trends of low visibility, haze and fog are influenced by the variation of many factors such as pollutant emissions, aerosol compositions and meteorological conditions, etc. During the past 30 years, the NCP has undergone rapid economic developments accompanied by growing energy consumptions. In the past decade, policies were made to reduce pollutant emissions in the NCP in hope to improve the air quality. In this section, the decadal trends of low visibility, haze and fog days will be examined to show the combined effect of various influencing factors.

3.2.1 The decadal trends of low visibility, haze and fog

The decadal variations of the annual and the 10 year moving average occurrence count of low visibility, haze and fog days during 1981–2010 are displayed in Fig. 3b. Before 1995, due to the rapid economic development, the increasing energy consumption has led to increasing numbers of haze and fog days, which resulted in more frequent low visibility events. During 1995–2003, with the development and employment of waste gas processing techniques, occurrence counts of low visibility, haze and fog days have entered a steady stage. After 2003, in preparation for the 2008 Beijing Olympic Games, under the influence of emission control policies, the number of low visibility, haze and fog days have drastically dropped. The variation trend of low visibility and haze days agrees well with that of the SO_2 emissions (Fig. 3a), suggesting that the control in emissions during the last decade effectively led to the decline of visibility and haze days.

The 10 year moving linear slopes of low visibility, haze and fog occurrence days during 1981–2010 are shown Fig. 3c. The maximum increasing slope for haze events can be found between 1989–1998, reaching 17 days 10 a^{-1}. After the period of 1994–2003, haze events have been mostly declining, reaching a maximum decreasing slope of 11 days 10 a^{-1} during 1996–2005. After 1987–1996, fog occurrences displays discontinuous decreasing trends. Major decreases happened during the periods of

1990–1999 and 2001–2010, with slopes of 10 days 10 a^{-1}. The count of low visibility days were increasing before the period of 1996–2005, with a maximum slope of 17 days 10 a^{-1} during 1983–1992. Afterwards, low visibility events were found to be less frequent, the maximum decreasing slope was found during 2001–2010, reaching 16 days 10 a^{-1}.

Generally, the occurrence frequency of low visibility, haze and fog in the NCP have all increased during 1980–1990. Under the effort of SO_2 emission reduction during the past few years, occurrence frequencies of low visibility, haze and fog have all decreased back to a similar level as in 1980.

3.2.2 The season-decadal trends of low visibility, haze and fog

Low visibility, haze and fog are strongly influenced by meteorological conditions, which in the NCP vary distinctly with season. This may cause different decadal variation in different seasons. Figure 4 shows the season-decadal variation trends of low visibility, haze and fog occurrence frequencies during 1981–2010.

During the past 30 years, haze events were most common during the heating season (Nov-Mar) and most rare during the end of spring and early autumn (Fig. 4d). After 1990, haze events started to appear not only during the heating season but also during summertime (Fig. 4b2). From the 10 year moving average occurrence frequencies of haze in spring, summer, autumn and winter (Fig. 4b1) it can be seen that summertime haze occurrence frequencies has been continuously increasing in the past 3 decades, while that in wintertime has been declining since 1995. In the past, heating processes during winter has led to high emissions of soot, which were responsible for the degradation of visibility. With the development of central heating and waste gas processing techniques, emissions by heating processes have been gradually declining, leading to less haze events during winter. However, atmospheric pollution has become more complex during recent years. During summer, the atmosphere becomes highly oxidative, aerosol pollution coexists with high concentrations of O_3 and VOCs (Ran et al., 2011),

ACPD
14, 16123–16149, 2014

which contribute to the fast aging and secondary formation of aerosols. Aged aerosols are more hygroscopic and can easily lead to haze events under suitable RH conditions (Chen et al., 2012).

Fog events appear most frequently during winter and most rarely during spring until early summer. The fog occurrence frequency during the past 30 years shows no significant variation trend in spring and summer, but shows a declining trend during winter after 1990 (Fig. 4c1).

Low visibility events are caused by both haze and fog. Their combined effect has resulted in high occurrence frequencies of low visibility during winter and lower ones during spring and summer (Fig. 4a1). Low visibility events during summertime has been continuously increasing in the past 3 decades, while those during spring, autumn and winter has been decreasing after 2000.

In all, wintertime low visibility, haze and fog days have been declining, while summertime low visibility and haze days have been increasing due to the variation in aerosol composition and the summertime high RH that favors the hygroscopic growth of particles.

3.3 The impact of wind on low visibility, haze and fog

3.3.1 The impact of wind on haze

Wind direction can influence the transport of pollutants, thus determining the spatial distribution of visibility degrading pollutants. Wind speed greatly influences the atmospheric stability and the atmospheric dispersion abilities. Low wind speeds suggest that the atmosphere is rather stable and the dispersion of local emissions is prohibited.

Figure 5a shows the spatial distribution of the average 14:00 LT surface wind direction during May–December 2009 in the entire NCP. The Yan and Taihang Mountains are governed by northwest winds, while the plain area is dominated by winds from the south. Along the south-western edge of the Taihang Mountains, the winds all come from the south-eastern direction, which can transport the emitted pollutants from the eastern part of the plain area to the western part. The weak north-western winds in the mountains block the way of the pollutant transport, leading to the accumulation of heavy loadings of aerosol and its precursors along the foot of the Taihang Mountains. This explains why haze events are most common in this region.

Figure 6a displays the distribution of the average 14:00 LT wind speed during 1981–2010. Average wind speeds at 14:00 LT decreases from the southeast to the northwest. Lowest values are found in the northwest corner, reaching below 3 $m\,s^{-1}$, while similar values were also detected in Xingtai and Handan, two heavily polluted cities in the southern corner. Average wind speeds near the coast (in the vicinity of Cangzhou) and in the southeast corner are large, reaching over 5 $m\,s^{-1}$. The low wind speeds are caused primarily by the Taihang Mountains, which slow down westerly winds before they reach the plain region. As can be seen from Fig. 5, the geographic height of the Taihang Mountains is higher in the north and lower in the south, which explains why wind speeds are lowest in the northwest corner. Another factor influencing the surface wind speed is the surface roughness. Large cities with densely distributed high buildings will add to the surface roughness and slow down near surface winds.

Although dispersion abilities are weakest in the northwest corner, due to relatively lower pollutant emissions in the mountain areas, low visibility and haze events are rare on the northwestern edge. However, the area near Baoding, where the pollution level is slightly higher than the mountain areas and distinctively lower than the polluted region in the southwest, is heavily affected by the low wind speeds, showing frequently occurring low visibility and haze events. The southwestern edge of the southern NCP region suffers from high pollutant emissions and is under relatively weak dispersion conditions. The low average wind speed centers in Shijiazhuang, Xingtai and Handan (Fig. 7a) conform to the high haze day count centers (Fig. 2c).

Figure 6b shows how the linear slope of the annual wind speed during 1981–2010 is distributed in the southern NCP. Over the entire region, wind speeds have been decreasing in the past 30 years. Large decreasing slopes were found in those regions with large average wind speeds, but also in parts of the northeast corner and in Shijiazhuang, which is the capital of Hebei Province. The regional average 10 year decreasing slope reaches 0.2 $m\,s^{-1}$ $10\,a^{-1}$, while that in Shijiazhuang reaches over 0.2 $m\,s^{-1}$ $10\,a^{-1}$ (Fig. 6c). The decrease in wind speed suggests that the atmosphere has become more stable and dispersion abilities has weakened throughout the entire region, which calls for even harder efforts to control emissions in order to prevent haze events.

3.3.2 The impact of wind on fog

The formation of fog needs a supersaturated water vapour environment, which requires favourable meteorological conditions. Figure 5b shows the average 08:00 LT 1000 hPa wind field during a continuous fog event that occurred between the 9 and 19 December 2002. Due to the topography of the NCP, an orographic wind convergence line going from southwest to the northeast is formed as indicated by the red line in Fig. 5b. The wind convergence line is also parallel to the ridge of the Taihang Mountains, coinciding with the zone with the most frequent fog events (Fig. 2d). Fog events usually occur during the night, when the mountain areas cool off faster than the plain area, forming a temperature gradient. To the west of the convergence line, near surface winds are dominated by cold north-westerly mountain winds, while to the east of the convergence line, surface winds are north-easterly or south-easterly. With the north-easterly winds comes the warm humid air from the Bohai Sea, while the south-easterly path is the most typical water vapour transport passage way for the entire NCP region. The wind convergence zone will hence favour the accumulation and convergence of water vapour, and lead to the formation of fog in this area.

3.4 The impact of RH on low visibility, haze and fog

The ambient RH can influence the visibility by affecting the hygroscopic growth and scattering abilities of atmospheric aerosols. Chen et al. (2012) suggest that, under RH $< 80\,\%$, visibility is highly dependent on dry aerosol volume concentrations, only under high aerosol loadings does the hygroscopic growth become important for visibility impairment. While for RH greater than 80 %, the hygroscopic growth of aerosols can greatly affect visibility, even under average aerosol pollution levels.

The 14:00 LT RH values that were accompanied by haze events (haze event RH) were sorted out and its occurrence frequency in the range of RH < 50 %, 50 % < RH < 60 %, 60 % < RH < 70 % and RH > 70 % was calculated for each station in each month during 1981–2010. Figure 7a2–d2 shows the regional average season-decadal variation of the occurrence frequency of haze event RHs. It can be noted that haze events mostly occur under RH > 60 % during summer and early autumn, while during late autumn, winter and spring, haze events mostly occur under RH < 60 %. This suggests that haze events during the warm season are caused both by high aerosol loadings and their hygroscopic growth, while those in the cold seasons are mostly induced by high aerosol loadings.

The occurrence frequency of haze events under low RH (RH < 50 %) in autumn, winter and spring has decreased over the past 30 years, with a slight rebound in the winter time data at the end of the last decade. This indicates that aerosol loadings during winter has declined, which could be the result of effective emission control measures during heating seasons. The occurrence frequency of haze events under higher RH (RH > 60 %) in autumn, winter and spring show increasing trends during the past 30 years. A possible cause could be the fact that atmospheric pollution has become more complicated over the years, leading to a higher fraction of secondary aerosols, which are more hygroscopic and are more likely to impair visibility through hygroscopic growth processes.

To further study if this phenomenon exists throughout the entire region, the decadal variation of haze event RH, annual average RH and annual haze days at four representative stations were analysed as is depicted in Fig. 9. The RH associated with haze events are typically higher than the average RH values. Zanhuang station shows continuously increasing number of haze days throughout the past 30 years, while Hengshui displays a continuous decline throughout the past 20 years (Fig. 9b). Shijiazhuang and

Longyao have both undergone an increase before 2000 and a decrease thereafter. Significant increasing trends can be found in the ratio of haze event RH and average RH at all four stations (Fig. 9a). This means that a higher fraction of the haze events are now caused by the hygroscopic growth of aerosols. The reduction in primary aerosol emissions further amplifies this effect.

4 Summary

In this study, the spatial distribution and decadal variation of low visibility, fog and haze events in the most polluted southern part of the NCP during the past 30 years were analysed and the impact of wind and RH on those events was investigated.

Haze and fog are distinctly distributed, which was determined by the topography of the NCP and the distribution of wind speed and wind direction. Haze occurs mostly along the south-western edge of the plain region, while fog mostly occurs within the central band area parallel to the ridge of the Taihang Mountains.

Annual low visibility, haze and fog days have shown increasing trends before 1995, have entered a steady stage during 1995–2003 and have drastically dropped thereafter during the preparation stage for the Beijing Olympic Games in 2008. Low visibility, haze and fog events all occurred most frequently during the heating season in the past 3 decades. Wintertime haze and fog both show decreasing trends, benefiting from the improvements in central heating and desulfurization techniques. Summertime haze, however, displayed continuous increasing trends during 1981–2010.

Both the distribution of the wind field and the decadal variation of wind speeds have great impacts on the occurrence of low visibility, haze and fog events. South-easterly winds in the southern part of the NCP which are blocked by the weak north-western winds in the Taihang Mountains has resulted in high pollutant concentrations along the foot of the mountain, which has led to frequent haze events. The orographic wind convergence zone parallel to the ridge of the Taihang Mountains in the central band area of the southern NCP was responsible for the frequent fog events in this region.

ACPD
14, 16123–16149, 2014

Wind speed has been decreasing throughout the entire southern NCP, resulting in more stable atmospheric conditions and weaker dispersion abilities, which calls for even harder efforts to control emissions in order to prevent haze events.

Haze events were strongly influenced by the ambient RH. Under RH below 60 %, haze events mostly occurred during the heating seasons, while for RH above 60 %, haze events were more likely to happen during summertime. Although annual RH values displayed no significant trends within the past 30 years, those RH values associated with haze days were evidently increasing, suggesting that an increasing fraction of haze events are caused by the hygroscopic growth of aerosols, rather than simply by high aerosol loadings.

Acknowledgements. This work is supported by the National 973 project of China (2011CB403402), the National Natural Science Foundation of China under Grant No. 41375134, the Beijing Natural Science Foundation (8131003), the Beijing municipal science and technology plan project No. Z131100006113013.

References

Chang, D., Song, Y., and Liu, B.: Visibility trends in six megacities in China 1973–2007, Atmos. Res., 94, 161–167, doi:10.1016/j.atmosres.2009.05.006, 2009.

Chen, J., Zhao, C. S., Ma, N., Liu, P. F., Göbel, T., Hallbauer, E., Deng, Z. Z., Ran, L., Xu, W. Y., Liang, Z., Liu, H. J., Yan, P., Zhou, X. J., and Wiedensohler, A.: A parameterization of low visibilities for hazy days in the North China Plain, Atmos. Chem. Phys., 12, 4935–4950, doi:10.5194/acp-12-4935-2012, 2012.

China Statistical Yearbook: http://www.stats.gov.cn/tjsj/ndsj/ (last access: 26 March 2014), 1995–2010.

Danielson, J. J. and Gesch, D. B.: Global multi-resolution terrain elevation data 2010 (GMTED2010), US Geological Survey Open-File Report 2011-1073, 26, 2011.

Deng, J., Du, K., Wang, K., Yuan, C.-S., and Zhao, J.: Long-term atmospheric visibility trend in Southeast China, 1973–2010, Atmos. Environ., 59, 11–21, doi:10.1016/j.atmosenv.2012.05.023, 2012.

Doyle, M. and Dorling, S.: Visibility trends in the UK 1950–1997, Atmos. Environ., 36, 3161–3172, doi:10.1016/S1352-2310(02)00248-0, 2002.
Fu, C. and Wu, J.: The different characteristics of sunny visibility over southwest china in recent 50 years, Procedia Environmental Sciences, 10, Part A, 247–254, doi:10.1016/j.proenv.2011.09.041, 2011.
Liu, H. J., Zhao, C. S., Nekat, B., Ma, N., Wiedensohler, A., van Pinxteren, D., Spindler, G., Müller, K., and Herrmann, H.: Aerosol hygroscopicity derived from size-segregated chemical composition and its parameterization in the North China Plain, Atmos. Chem. Phys., 14, 2525–2539, doi:10.5194/acp-14-2525-2014, 2014.
Ma, N., Zhao, C. S., Nowak, A., Müller, T., Pfeifer, S., Cheng, Y. F., Deng, Z.Z., Liu, P. F., Xu, W. Y., Ran, L., Yan, P., Göbel, T., Hallbauer, E., Mildenberger, K., Henning, S., Yu, J., Chen, L. L., Zhou, X. J., Stratmann, F., and Wiedensohler, A.: Aerosol optical properties in the North China Plain during HaChi campaign: an in-situ optical closure study, Atmos. Chem. Phys., 11, 5959–5973, doi:10.5194/acp-11-5959-2011, 2011.
Molnár, A., Mészáros, E., Imre, K., and Rüll, A.: Trends in visibility over Hungary between 1996 and 2002, Atmos. Environ., 42, 2621–2629, doi:10.1016/j.atmosenv.2007.05.012, 2008.
Ran, L., Zhao, C. S., Xu, W. Y., Lu, X. Q., Han, M., Lin, W. L., Yan, P., Xu, X. B., Deng, Z. Z., Ma, N., Liu, P. F., Yu, J., Liang, W. D., and Chen, L. L.: VOC reactivity and its effect on ozone production during the HaChi summer campaign, Atmos. Chem. Phys., 11, 4657–4667, doi:10.5194/acp-11-4657-2011, 2011.
Schichtel, B. A., Husar, R. B., Falke, S. R., and Wilson, W. E.: Haze trends over the United States, 1980–1995, Atmos. Environ., 35, 5205–5210, doi:10.1016/S1352-2310(01)00317-X, 2001.
Vautard, R., Yiou, P., and van Oldenborgh, G. J.: Decline of fog, mist and haze in Europe over the past 30 years, Nat. Geosci., 2, 115–119, doi:10.1038/ngeo414, 2009.
Wu, J., Fu, C., Zhang, L., and Tang, J.: Trends of visibility on sunny days in China in the recent 50 years, Atmos. Environ., 55, 339–346, doi:10.1016/j.atmosenv.2012.03.037, 2012.
Xu, W. Y., Zhao, C. S., Ran, L., Deng, Z. Z., Liu, P. F., Ma, N., Lin, W. L., Xu, X. B., Yan, P., He, X., Yu, J., Liang, W. D., and Chen, L. L.: Characteristics of pollutants and their correlation to meteorological conditions at a suburban site in the North China Plain, Atmos. Chem. Phys., 11, 4353–4369, doi:10.5194/acp-11-4353-2011, 2011.

Zhao, P., Zhang, X., Xu, X., and Zhao, X.: Long-term visibility trends and characteristics in the region of Beijing, Tianjin, and Hebei, China, Atmos. Res., 101, 711–718, doi:10.1016/j.atmosres.2011.04.019, 2011.

ACPD
14, 16123–16149, 2014

Table 1. The number (percentage) of stations under various count ranges of low visibility, haze and fog days during 1981–2010.

	Days					
Stations	≥ 3000	2000–2999	1000–1999	500–999	100–499	< 100
Low Visibility	2 (3 %)	6 (9 %)	22(34 %)	23 (36 %)	11 (17 %)	0 (0 %)
Haze	0 (0 %)	2 (3 %)	12(19 %)	15 (23 %)	30 (47 %)	5 (8 %)
Fog	0 (0 %)	0 (0 %)	8 (13 %)	47 (73 %)	9 (14 %)	0 (0 %)

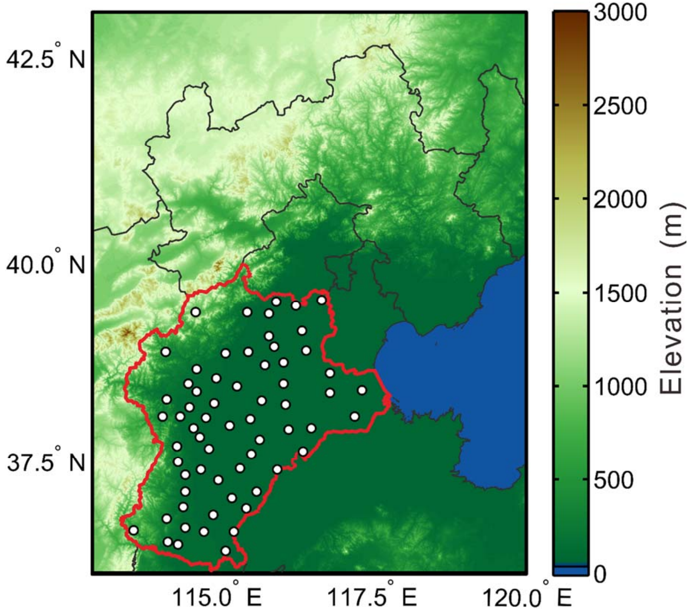

Figure 1. The location of the measurement sites (circle), the area of study (red line) and the regional topography by (Danielson and Gesch, 2011) (color).

ACPD
14, 16123–16149, 2014

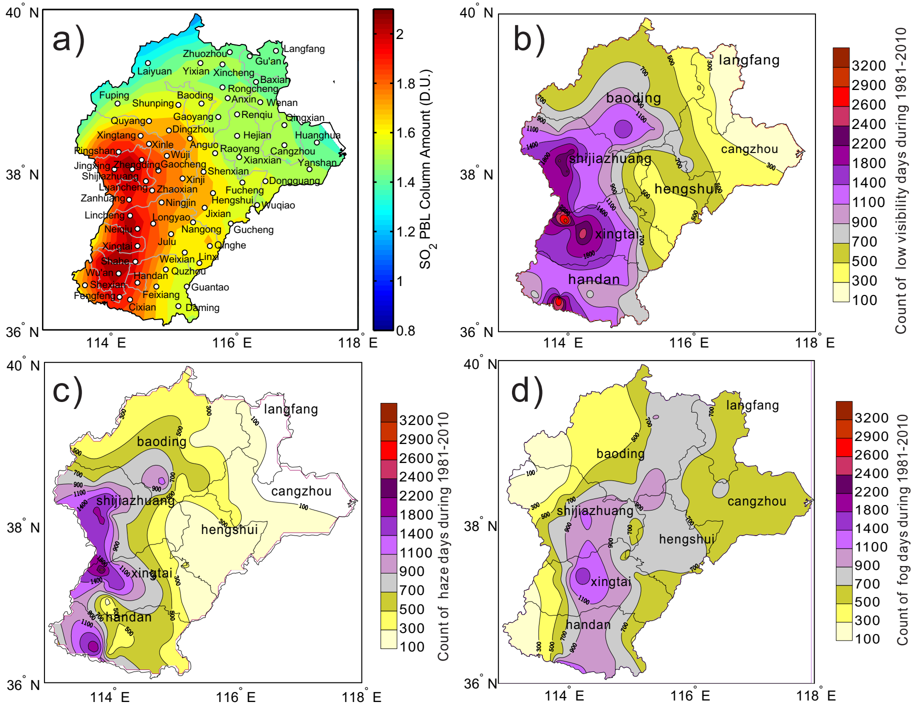

Figure 2. (a) Average OMI SO_2 PBL column amount during 2005–2012 with the location of the 64 stations and the count of **(b)** low visibility, **(c)** haze and **(d)** fog days during 1981–2010 in the southern NCP.

ACPD
14, 16123–16149, 2014

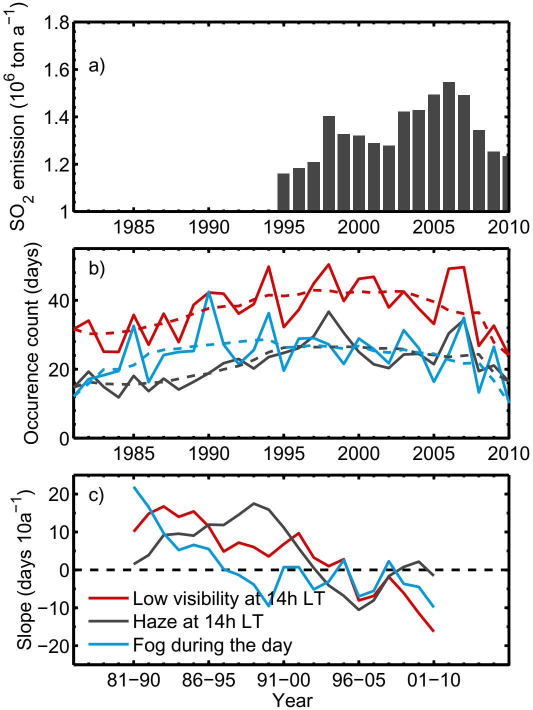

Figure 3. (a) The annual SO_2 emissions in Hebei Province inferred from the China statistical yearbooks (National Bureau of Statistics of China, 1995–2010); **(b)** the annual (solid lines) and the 10 year moving average (dashed lines) occurrence count of low visibility, haze and fog days among the 64 stations during 1981–2010; **(b)** the 10 year moving linear slope of the annual average occurrence count of low visibility, haze and fog days among the 64 stations during 1981–2010.

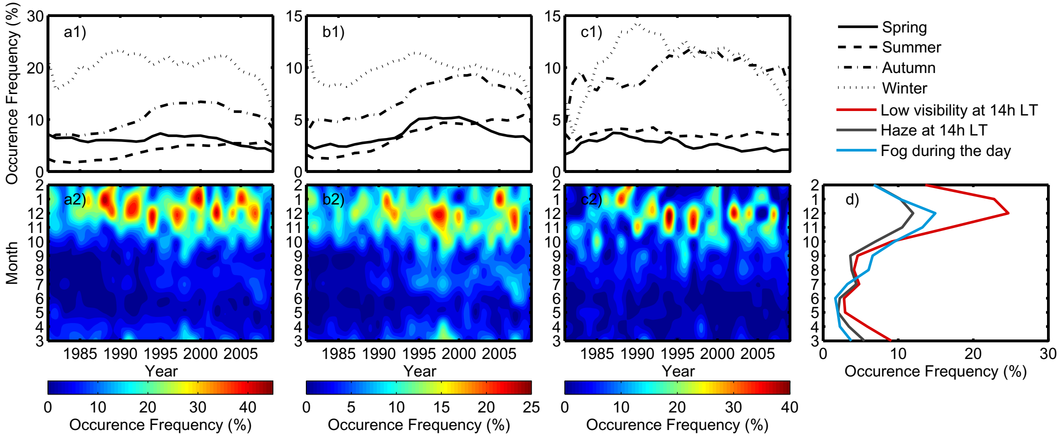

Figure 4. (1) The trend of the 10 year moving average occurrence frequency of **(a)** low visibility events at 14:00 LT, **(b)** haze events at 14:00 LT and **(c)** fog events during the day among the 64 stations during spring (MAM), summer (JJA), autumn (SON) and winter (DJF); **(2)** The season-annual variation of the average occurrence frequency of **(a)** low visibility events at 14:00 LT, **(b)** haze events at 14:00 LT and **(c)** fog events during the day among the 64 stations and **(d)** the seasonal variation of the average occurrence frequency of low visibility events at 14:00 LT, haze events at 14:00 LT and fog events among the 64 stations during 1981–2010.

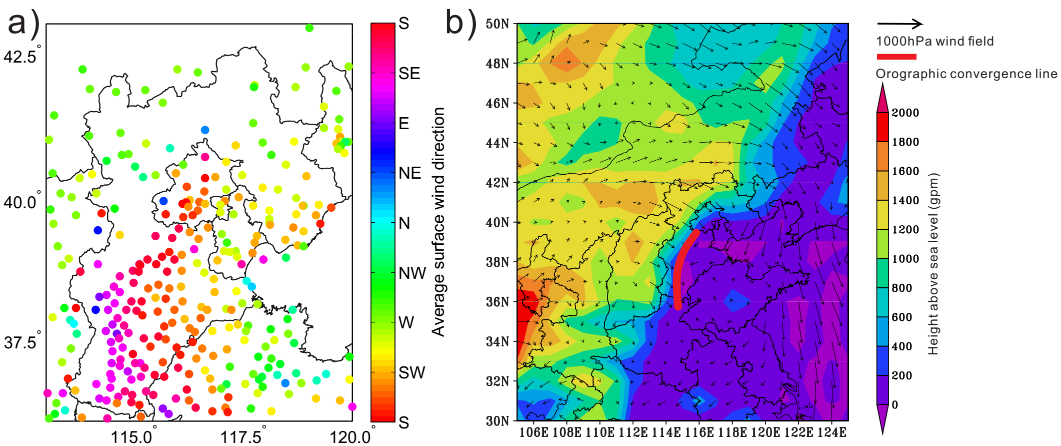

Figure 5. (a) Averaged 14:00 LT surface wind direction during May–December 2009 given by 307 AWS stations. **(b)** The orographic height a.s.l. (shading), the average 08:00 LT 1000 hPa NCEP final analysis wind field (black arrows) and the orographic convergence line (red line) during a continuous fog event during 9–19 December 2002.

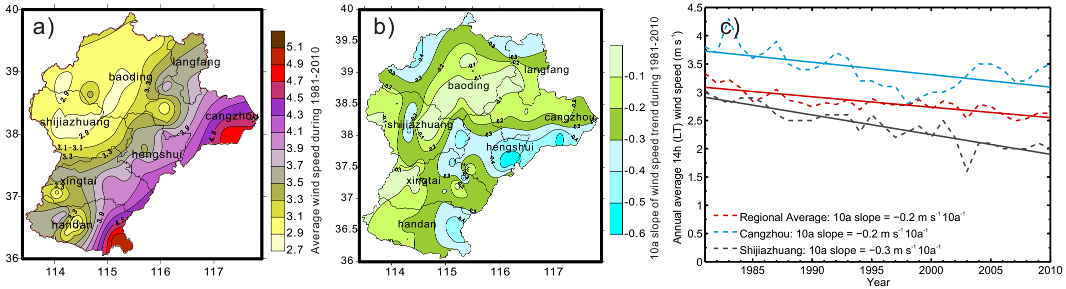

Figure 6. (a) Distribution of the average 14:00 LT wind speed during 1981–2010 in the southern NCP; **(b)** distribution of the linear slope of the annual wind speed during 1981–2010 in the southern NCP; **(c)** Variation (dashed lines) and linear trend (solid lines) of the regional average 14:00 LT wind speed and that of Cangzhou and Shijiazhuang during 1981–2010.

ACPD
14, 16123–16149, 2014

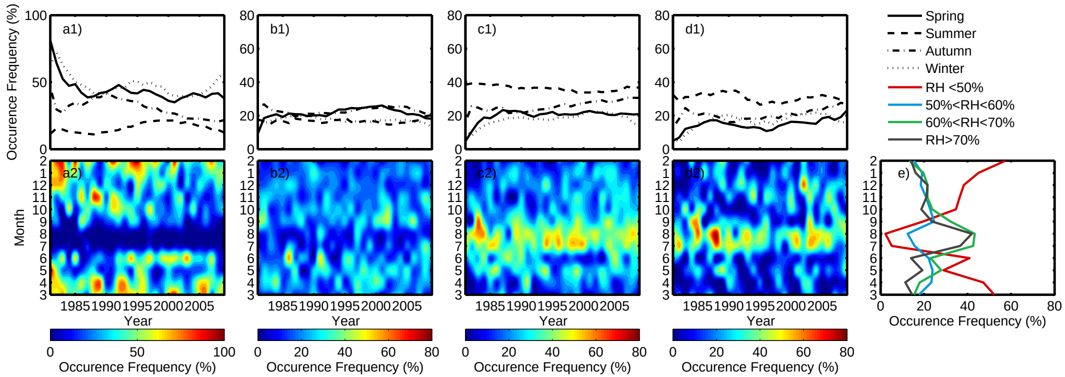

Figure 7. (1) The decadal trend of the 10 year moving average occurrence frequency of 14:00 LT haze event RH in the range of **(a)** RH < 50 %, **(b)** 50 % < RH < 60 %, **(c)** 60 % < RH < 70 % and **(d)** RH > 70 % during spring (MAM), summer (JJA), autumn (SON) and winter (DJF); **(2)** The season-decadal variation of the occurrence frequency of 14:00 LT haze event RH in the range of **(a)** RH < 50 %, **(b)** 50 % < RH < 60 %, **(c)** 60 % < RH < 70 % and **(d)** 70 % < RH < 80 % and **(e)** the seasonal variation of the average occurrence frequency of 14:00 LT haze event RH in the range of **(a)** RH < 50 %, **(b)** 50 % < RH < 60 %, **(c)** 60 % < RH < 70 % and **(d)** RH > 70 % during 1981–2010.

ACPD
14, 16123–16149, 2014
The distribution and trends of fog and haze
G. Q. Fu et al.

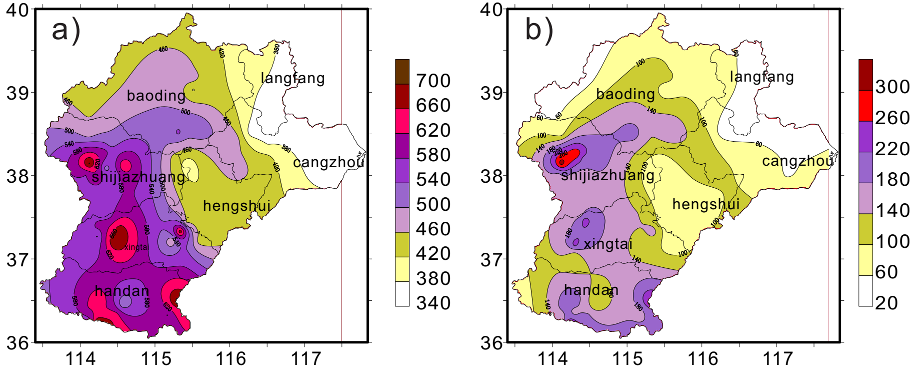

Figure 8. The distribution of **(a)** the total average 14:00 LT RH and **(b)** the average 14:00 LT RH on haze days during 1981–2010 in the southern NCP.

ACPD
14, 16123–16149, 2014

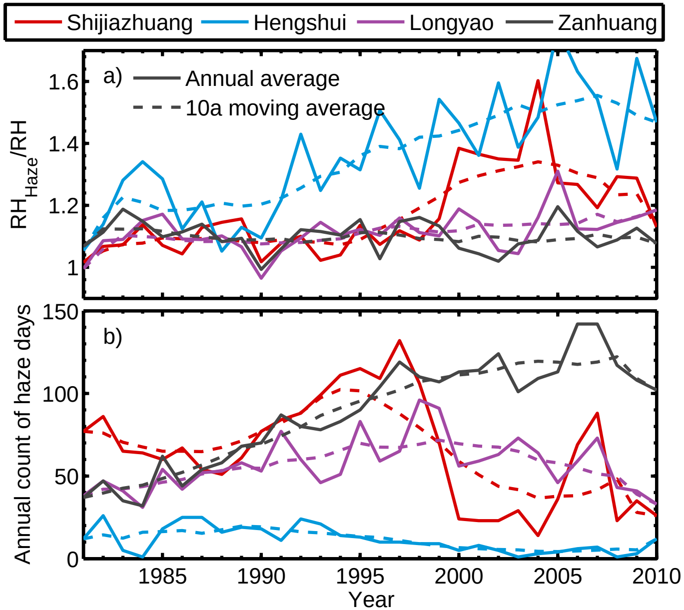

Figure 9. (a) The decadal variation of the haze event associated RH divided by the average RH and **(b)** the annual count of haze days during 1981–2010 at Shijiazhuang, Hengshui, Longyao and Zanhuang.

ACPD
14, 16123–16149, 2014

Title Page
Abstract | Introduction
Conclusions | References
Tables | Figures
◀| |▶
◀ ▶
Back | Close
Full Screen / Esc
Printer-friendly Version
Interactive Discussion